Catalysis Today 154 (2010) 256–263

Contents lists available at ScienceDirect

Catalysis Today

journal homepage: www.elsevier.com/locate/cattod

Hydroprocessing catalyst deactivation in commercial practice

Bas M. Vogelaar*, Sonja Eijsbouts, Jaap A. Bergwerff, Johan J. Heiszwolf

Albemarle Catalysts, PO Box 37650, 1030 BE Amsterdam, the Netherlands

ARTICLE INFO

Article history:
Available online 27 April 2010

Keywords:
Hydroprocessing
Oil refining
Deactivation
Sintering
Coke
Metal deposition

ABSTRACT

Hydroprocessing catalysts are susceptible to deactivation by several mechanisms, e.g. coke formation, metals deposition and active phase sintering, in their life cycle. Typical examples of catalyst deactivation are presented, showing the phenomena that may be encountered in commercial hydroprocessing units. Spent samples of hydroprocessing catalysts were obtained from various commercial units, as well as pilot plants. The cause(s) of deactivation were identified by analyzing spent catalyst samples for coke and metal content, pore size distribution and the distribution of metals (by SEM-EDX and STEM-EDX). Catalysts applied in the hydroprocessing of light feeds (middle distillates) mainly deactivate due to coke deposition and possibly sintering. Poisoning by metal deposition becomes significant during hydroprocessing of heavy feeds (like VGO and residue) as well as upgraded streams (e.g. coker products). Once the possible causes are known, deactivation mitigation strategies can be defined, which comprise optimizing the catalyst properties, catalyst loading and reactor operation.

1. Introduction

Hydroprocessing is a key technology for the production of clean fuels in today's refinery operations. It comprises a wide variety of reactor systems (fixed bed, moving bed, and ebullated bed), feeds (middle distillates, vacuum gas oil, residue) and operating conditions (gas/liquid phase, low and high temperatures, low and high pressures). Although this process is over 70 years old, it is still subject to continuing changes [1]. Over the years, refineries have been processing heavier and more sour feeds, due to shifting crude diversity and sources. These crudes contain more contaminants and require a higher conversion level, which has lead to the development of improved hydroprocessing catalysts tailored for such applications. The catalysts, which are mostly based on Ni, Co, Mo and W sulfides, are susceptible to several deactivation mechanisms during their life cycle [2]. Catalyst deactivation will become more and more critical, due to the ongoing trend in increasing hydroprocessing severity and maximizing catalyst performance.

Catalyst deactivation plays an important role in process design and operation within the petrochemical industry. Various chemical reaction engineering solutions can be applied depending on the typical lifetime of the catalyst. A classical example is the fluid catalytic cracking process. The FCC catalyst must be continuously regenerated due its very short lifetime [3]. In most hydroprocessing applications, the life of the catalyst is long enough to enable the use of fixed-bed reactors. This implies that the process needs to be periodically taken offline to replace the spent catalyst. The loss of unit availability is often minimized by combining the moment of catalyst change out with the periodic maintenance of the unit [4]. Consequently, the ability to control the catalyst life cycle length is crucial for refinery management.

The HPC catalyst life cycle is strongly influenced by the type of application. Fig. 1 shows typical catalyst deactivation curves for different classes of feeds. The processing of heavier feeds requires higher operating temperatures (and pressures), which is generally accompanied by a faster deactivation rate of the catalyst. This results in a shorter cycle length, although the higher pressure somewhat alleviates the deactivation. The intrinsic mechanisms of catalyst deactivation can be classified into three basic types of processes: chemical, mechanical and thermal [5]. In hydroprocessing, each class is represented respectively by the following deactivation mechanisms: active site coverage by strongly adsorbed species and deposits (coke and metals), pore mouth constriction/pore blockage and sintering of the active phase [6]. A better understanding of deactivation could extend catalyst life and thus have enormous economic benefits.

Ideally, catalysts should be studied under industrially relevant conditions. It is however difficult to mimic these conditions in laboratory experiments, because the deactivation of hydroprocessing catalysts takes place on a very long time scale. That is why the investigation of samples withdrawn from an industrial or pilot reactor can provide information of great value [7]. The aim of the present study is to show the deactivation behavior of commercial hydroprocessing catalysts under typical industrial conditions. Spent hydroprocessing catalysts were retrieved from several commercial and pilot units and a series of samples was selected for

* Corresponding author.
E-mail address: bas.vogelaar@albemarle.com (B.M. Vogelaar).

0920-5861/$ – see front matter © 2010 Elsevier B.V. All rights reserved.
doi:10.1016/j.cattod.2010.03.039

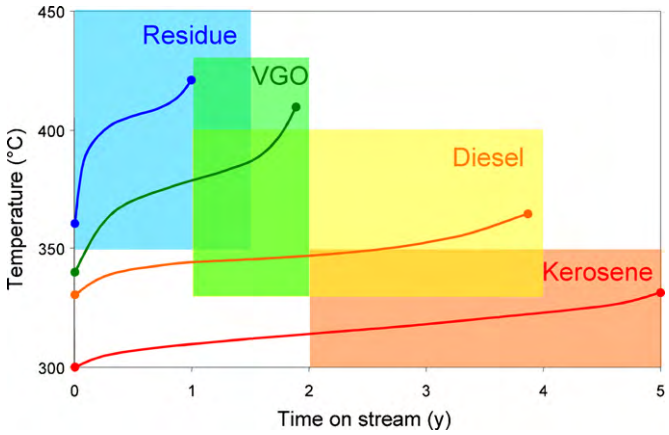

Fig. 1. Typical catalyst deactivation curves and operating cycle limits of hydroprocessing applications.

further investigation. These catalysts represent typical cases of catalyst deactivation in commercial practice. Using advanced analysis techniques, the mechanisms responsible for the deactivation of the catalysts can be identified, and options to mitigate catalyst deactivation can be defined.

2. Experimental

2.1. Spent catalyst samples

Several spent catalyst samples used in the hydroprocessing of diesel, vacuum gas oil (VGO) and vacuum residue were obtained from various industrial hydroprocessing reactors and/or pilot plants. Further details regarding the origin of the sample will be given in Section 3. Any remaining oil was removed from the catalyst particles by Soxlet extraction with toluene, prior to further analysis.

2.2. Elemental analysis, thermogravimetric analysis and porosimetry

The elemental composition of the spent catalysts was determined by XRF analysis using a Philips PW 2400 X-Ray fluorescence spectrometer, after calcining the samples at 450 °C. The total carbon content was measured using a LECO CS-200CSH apparatus. Thermogravimetric analysis (TGA) was carried out using a Mettler Toledo SDTA851 apparatus coupled with a Nicolet iS10 infrared off-gas analyzer. Nitrogen porosimetry measurements were performed using a Micromeretics GEMINI-V apparatus, after drying the samples under N_2 at 120 °C for 1 h. Mercury porosimetry measurements were performed using a Micromeretics AutoPore IV 9520 system.

2.3. Electron microscopy

The samples were evacuated for at least 2 h at 150 °C and subsequently vacuum impregnated with the standard mixture Ultra Low Viscosity Kit, hard version (Polaron Instruments Inc.). The mixture with catalyst was transferred into a polyethylene capsule (BEEM) and mixed with fresh embedding medium. The epoxy embedding medium was hardened at least 48 h under N_2 (2 bar, 60 °C).

For STEM-EDX analysis, sections of about 60 nm thickness were prepared using a Leica Reichert Ultracut-S ultramicrotome, collected on a water surface and transferred to a slightly etched (Ar plasma) Cu grid and dried. The thin sections on the TEM grid were covered with a thin layer of carbon to prevent charging during TEM analysis. Shortly after preparation, the sections were investigated with a JEOL JEM-2010F-HR TEM, with a 200 kV electron beam (Field Emission Gun, FEG), equipped with a STEM unit and a Thermo Noran EDX system. The active phase dispersion was studied by high resolution TEM imaging under slightly underfocussed conditions (−48 nm). The distribution of active metals was studied by STEM-EDX spectral imaging under analytical probe (1.0 nm) conditions.

For SEM-EDX analysis, a cross-section of an individual embedded extrudate was made using a diamond knife. The cross-section was mounted on a stub with conductive carbon cement (Leit C). A conductive carbon coating was deposited by a Balzers MED10 apparatus to avoid charging in the SEM. Micrographs were made by a Tescan analytical SEM and a LEO 1550 high resolution SEM. EDX spectra were obtained with an Oxford INCA system.

3. Results and discussion

3.1. Diesel HPC spent catalysts

In middle distillate applications (kerosene and diesel), the catalyst is typically very stable due to the relatively mild process conditions and light feedstock, with a typical boiling range between 220 and 350 °C. As a consequence, cycle length is usually very long (up to 5 years, Fig. 1). The most important factor involved in the catalyst deactivation is active site coverage by nitrogen compounds and coke [8]. Nitrogen-containing compounds are the most common poisons for hydroprocessing catalysts. Because of their basic nature, they adsorb reversibly or irreversibly on catalyst acidic sites, depending on reaction conditions. Irreversibly adsorbed species may eventually be converted to coke [9]. Coke deposition occurs in virtually all hydroprocessing applications. However, coke build-up increases with the boiling range and/or aromaticity of the processed feed [10]. Deactivation by coke is strongly influenced by operating conditions (temperature, partial pressure of hydrogen, % aromatic saturation and H_2/oil-ratio). Typically, coke is rapidly formed in the initial stage of the operation; then the coke level reaches a near steady-state, and increases again at the end of the cycle [11]. The catalyst may retain a substantial portion of its original activity in spite of the rapid initial coke deposition [12].

Two spent catalyst samples were selected from a commercial HPC unit and a pilot reactor processing ultra low sulfur diesel (ULSD). One catalyst was applied in a normal operating cycle, while the other was exposed to extreme process conditions, i.e. high temperatures, low pressures and high conversion levels, in order to accelerate the deactivation process(es). Aim of this artificial aging procedure was to compare the deactivation phenomena with a normal life cycle, by analyzing the spent catalysts. The catalyst deactivated more in the normal cycle than during the artificial aging run (about 25 °C difference). Options to measure coke deposition in a spent catalyst pellet on a detailed scale are limited [13], however, the properties of coke can be analyzed using conventional methods [14]. Fig. 2 shows the coke characterization using TGA-IR. The major part of the weight loss occurs in the region 250–550 °C where coke is combusted, as is apparent from the CO_2 signal. Both samples feature a peak maximum around 425 °C, in agreement with other reports [14,15]. The sample from the normal cycle shows the highest weight loss and CO_2 evolution in this region. Furthermore, the temperatures of the onset and completion of the coke combustion is about 50 °C higher for this sample as compared to the sample from artificial aging. Hence, it can be concluded that the spent sample from the normal cycle contains more coke, and that this coke is more refractory (i.e. more difficult to combust), which is in line with the observed difference in deactivation. This illustrates that time on stream is an important factor in the coking mechanism [11]; the relatively short artificial aging procedure results in

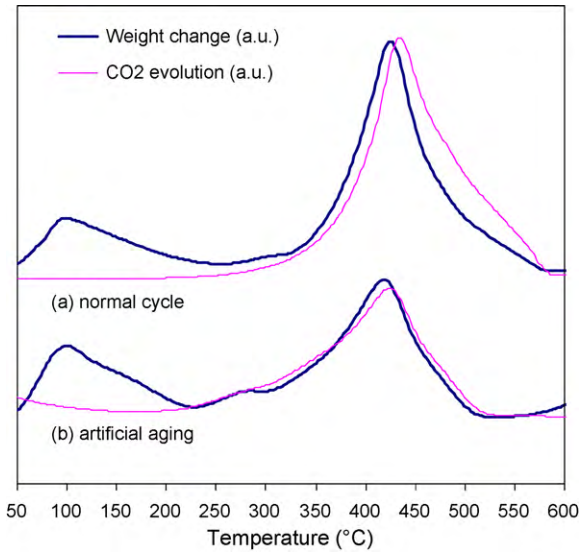

Fig. 2. TGA-IR analysis of coke deposits on spent ULSD catalysts after (a) normal cycle and (b) artificial aging.

"soft coke", which gets gradually converted into "hard coke" [2], as observed in the much longer normal operation cycle.

Besides coking, deactivation due to sintering may become an important factor, in particular near the end of the cycle when the catalyst operates at high temperatures. Prolonged exposure at elevated temperatures can lead to irreversible structural changes of the catalyst, causing a permanent activity loss. This may include sintering or segregation of the active phase, diffusion of active metals to the support and/or recrystallization of the metal phases [6]. The agglomeration of the active metals leads to a loss of active surface sites [16]. To investigate this deactivation process, both samples were studied using electron microscopy. Fig. 3 shows the distribution of active metals in the catalyst pellets, measured by STEM-EDX analysis. The spent sample from the normal cycle exhibits an even distribution of the active metals throughout the particle. Some fluctuations are observed, which follow the density variations of the alumina support material, envisaged by the distribution of aluminum. In contrast, the high-temperature exposed catalyst shows very distinct metal-rich areas in the STEM cross-section. According to the EDX analysis these domains comprise cobalt, molybdenum and sulfur. This indicates that the catalyst active phase has sintered to form larger agglomerates with a diameter of 100–400 nm.

The effect of sintering on a local scale is shown by the TEM micrographs in Fig. 4. The spent catalyst from the normal cycle has a relatively high dispersion, shown by the large number of short, individual MoS_2 slabs [17]. The dispersion of the high-temperature exposed catalyst shows signs of sintering. The length and very high stacking degree of the MoS_2 slabs indicate a very low dispersion. This loss of dispersion is expected to have a dramatic impact on the catalyst activity. Summarizing, the catalyst from the normal cycle shows no signs of extensive sintering, whereas the catalyst exposed to high temperatures is strongly sintered. This is the major cause of deactivation during the artificial aging run, whereas coking is mainly responsible for the catalyst deactivation during normal processing. Hence, it is concluded that the artificial aging treatment has resulted in a completely different deactivation behavior of the catalyst, as compared to the normal operation cycle. This illustrates that it is difficult to mimic the industrial life cycle of a catalyst on a laboratory scale, especially when conditions are used that strongly deviate from typical process operation [18].

Deactivation mitigation strategies for middle distillate applications are limited and focus on the use of mild operating conditions during both presulfiding and during the normal operation cycle. If the deactivation mechanism remains limited to coking and moderate sintering of the active metals phase then the catalyst may be regenerated or reactivated to activity levels close to that of the fresh catalyst [2].

3.2. VGO HPC spent catalysts

The hydroprocessing of vacuum gas oil (VGO) typically involves more severe conditions because the feedstock contains more refractory species. Also, VGO is much heavier than diesel, having a boiling range typically between 350 and 560 °C. The catalyst deactivates faster, which results in shorter cycle lengths (Fig. 1). Catalyst deactivation is also dependent on the target sulfur level, as lower levels of product sulfur require more severe operating conditions [19]. Next to deactivation by coke, metal deposition becomes an important factor in the hydroprocessing of VGO. Heavy oil fractions typically contain Ni and V organometallic compounds, e.g. porphyrin structures. During high-temperature reaction, these molecules decompose on the catalyst surface into Ni or V sulfides. This does not directly lead to a complete loss of activity, since these sulfides are able to catalyze hydroprocessing reactions to

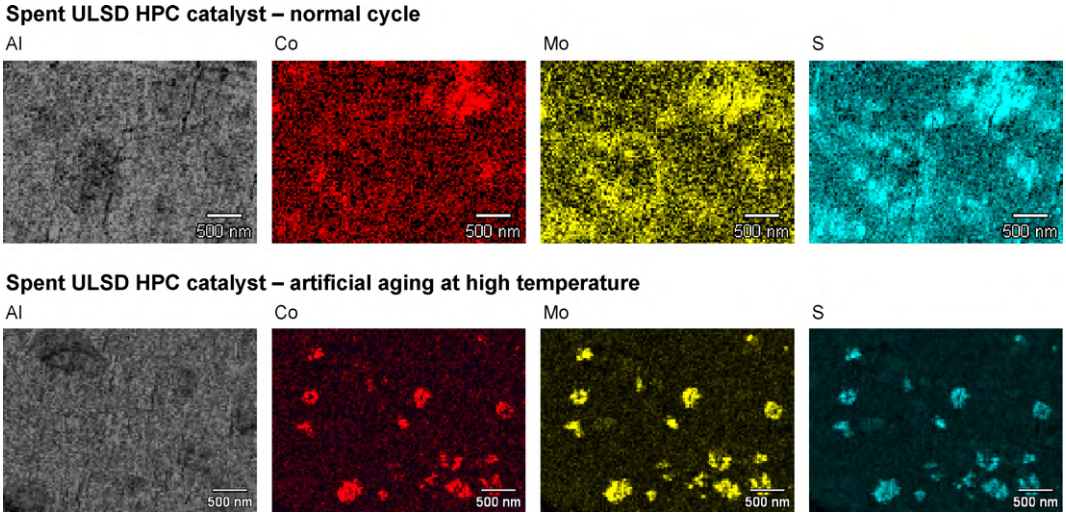

Fig. 3. STEM-EDX analysis of spent diesel HPC catalysts: distribution of active metals.

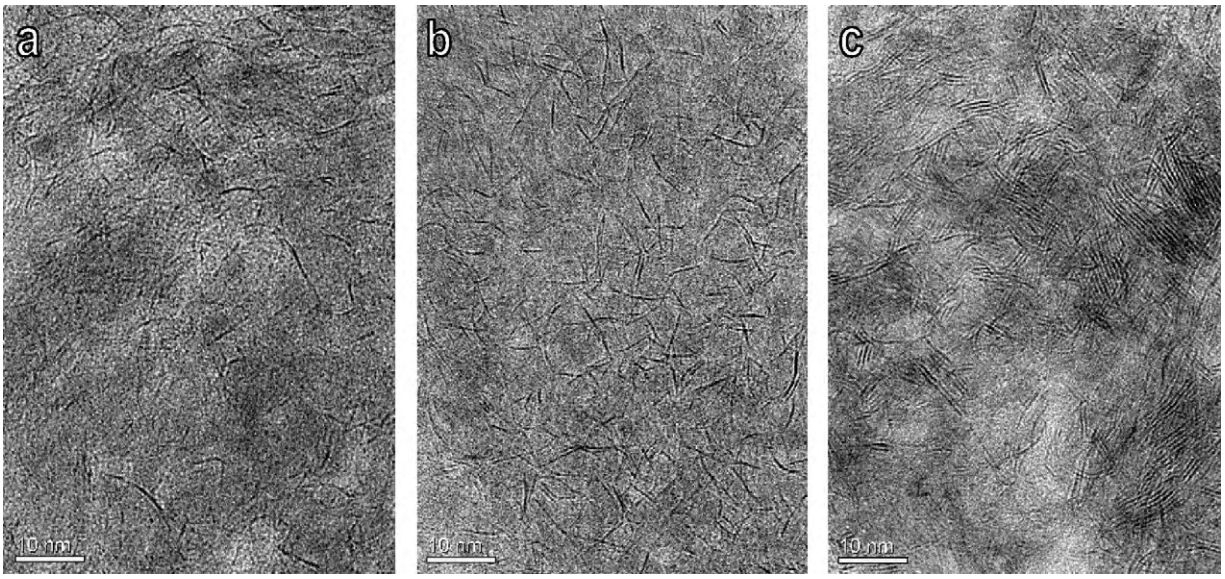

Fig. 4. High resolution TEM analysis of ULSD catalysts: dispersion of (a) fresh reference sample, (b) spent sample after normal cycle and (c) spent sample after artificial aging at high temperature.

Table 1
Spent VGO catalyst samples from different layers in the reactor: analysis of coke and metal contaminants.

	Guard bed	Layer 1	Layer 2	Layer 3	Layer 4	Layer 5
Coke (wt%)	14	11	9.8	9.5	12	15
SiO_2 (wt%)	8.0	5.5	4.2	4.0	3.0	2.2
NiO (wt%)	2.5	1.3	1.0	0.5	0.5	0.3
Fe (wt%)	0.5	0.2	0.5	0.2	0.0	0.0
V_2O_5 (wt%)	7.5	4.5	3.5	2.8	1.5	1.0

some extent [20]. However, deposition occurs preferentially at the edge of the catalyst pellets, because the diffusion rate is low. As the concentration of metals builds, pore mouth poisoning and pore blockage can occur [21]. Several other metal contaminants may be introduced by upstream operations [22], e.g. As from drilling fluids, Na from seawater, Si from antifoaming agents and Fe from corrosion. Although their concentration in the feed is relatively low, poisoning effects can be stronger than those of Ni and V.

Generally, the degree of deactivation and the dominating mechanisms depend on the position of the catalyst in the reactor [6]. Table 1 shows the distribution of deposited metals and coke on the spent catalyst as a function of position in the catalyst bed of an FCC pretreatment unit processing VGO. The amount of metals deposited on the catalyst decreases from inlet to outlet. The major part of the metal contaminants is picked up by the Demet guard bed at the top of the reactor. It should be noted that also the upper layer of the main catalyst bed may accumulate a significant amount of metals. As a result, catalyst re-use by regeneration is not possible, because for a successful activity recovery, total concentration of metal contaminants should be below about 2 wt%. This condition may be achieved by increasing the volume of guard bed catalyst at the expense of hydroprocessing activity, or by reducing the amount of feed processed. The cycle length is substantially shortened by both options; hence, the most cost-effective choice in VGO applications often is not to regenerate the catalyst [2]. The coke deposits on the catalyst shows a different trend: coke content at the top of the bed is high, then decreases toward the middle section, and increases again at the bottom. This can be explained by the different coking mechanisms playing a role: at the reactor inlet, the concentration of strongly adsorbing molecules and coke precursors is high, resulting in a fast coke build-up. Further down the catalyst bed, less coke is deposited because most coke precursors have been

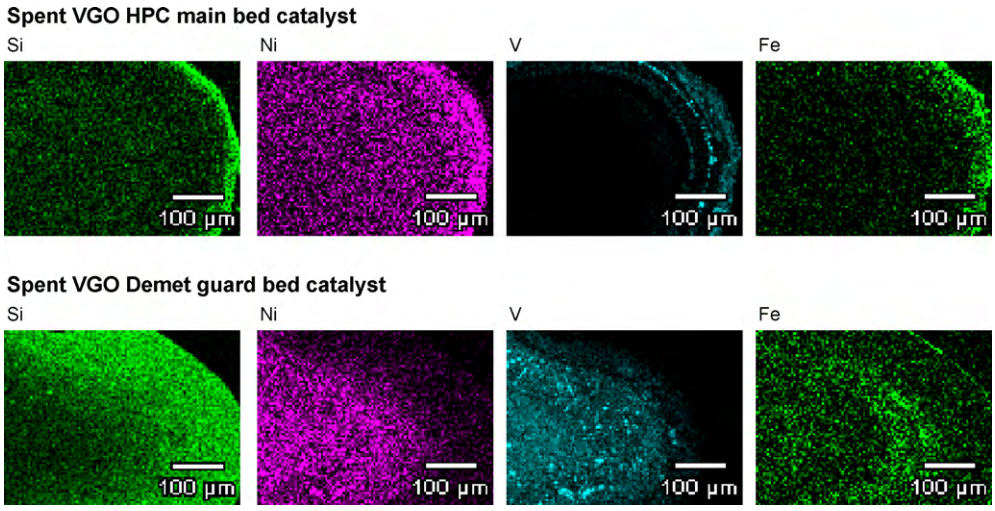

Fig. 5. SEM-EDX cross-section analysis of spent VGO HPC catalyst extrudates: distribution of typical contaminants.

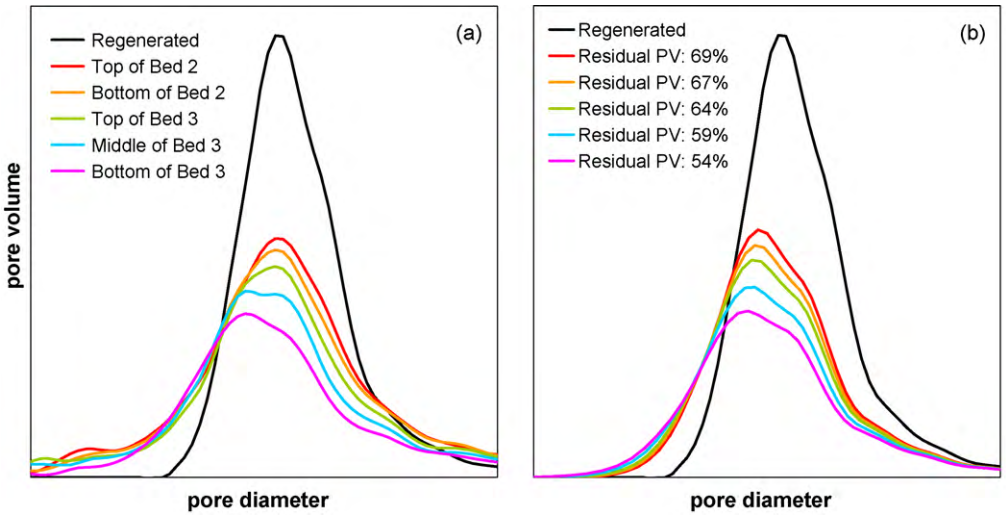

Fig. 6. Spent VGO catalyst samples from different positions in the reactor: (a) measured and (b) simulated effect of coke deposition on pore size distribution and pore volume (PV).

removed. However, temperature increases and hydrogen availability decreases towards the reactor outlet, which again results in a higher coke build-up in the bottom section of the catalyst bed due to dehydrogenation reactions [15].

Fig. 5 shows cross-sectional images of spent VGO hydroprocessing catalysts. The SEM-EDX element mapping indicates where different metals, present in the VGO feed, have deposited within the NiMo catalyst pellets. The external surface of the VGO HPC main bed catalyst is enriched in Si, Ni, V and Fe, which have deposited from the feed [23,24]. Fe mostly originates from corrosion products (Fe oxide and sulfide) in the field and during pipelining; some crudes also contain trace amounts of organic Fe compounds. Si mostly originates from antifoaming additives applied upstream in the refinery, e.g. in a coker unit [6]. To prevent deactivation of the main bed catalyst by metal deposition, a metal trapping catalyst is used as a guard bed. The pore structure and active phase of such catalysts is designed to enable the penetration of metal poisons into the catalyst pellet, for a maximum uptake capacity [23]. Fig. 5 also shows the metal pickup of a typical VGO Demet catalyst pellet. In this case, all metal contaminants have deposited throughout the particle.

Coke deposition plays a role in every hydroprocessing application, but the impact on deactivation increases with process severity and heavier feeds. Catalysts used in heavy feed hydroprocessing (VGO and residue) often exhibit pore plugging due to coke deposition [25]. This deactivation process can be visualized by comparing the pore size distribution of the used and regenerated catalysts. Fig. 6a shows the pore size distributions of another set of spent VGO catalyst samples from different positions in the reactor. The total pore volume of the spent catalysts has decreased considerably compared to the regenerated sample, indicating that part of the pore space is filled with coke. The volume occupied by the coke deposits increases towards the bottom section of the reactor, in agreement with the trend in the amount of coke previously shown (Table 1).

If all pores are well accessible, coke deposits will be evenly distributed over the catalyst active surface [26]. This results in a decrease in pore radius with increasing coke layer thickness. Fig. 6b shows the simulated effect of coke deposition on the pore size distribution, assuming cylindrical pore geometry. The layer thickness of the coke was varied to match the measured pore size distributions (Fig. 6a), in a range of 1–2 nm. These values agree with those reported in literature for similar cases [26,27]. The uniform coking model shows that more coke (thicker layers) results in lower total pore volume and smaller mean pore diameter. The simulated and measured distributions are very similar, although they do not perfectly overlap. This indicates a high probability of the suggested coking mechanism.

Deactivation mitigation strategies for VGO units focus mainly on the design of the guard bed system. Key purpose of the guard bed system is to effectively capture foulants to extend the catalyst life of the main bed. Because for the different foulants (As, Fe, Ni, Si V) the trapping mechanisms are different, custom Demet guard catalysts have been developed for each class of foulant. Depending on the composition of the feed and operating conditions of the unit, the size and composition of the guard bed system needs to be designed for each unit.

3.3. *Residue HPC spent catalysts*

Residue hydroprocessing is marked by very short catalyst lifetimes due to the extremely high severity required for processing these heavy feeds which initial boiling point exceeds 560 °C (Fig. 1). Furthermore, the level of contaminants in the feed (such as V and Ni) and its tendency to from coke is even higher than in VGO hydroprocessing. The catalyst mainly suffers from rapid coking and metal deposition, which plugs the pore structure. Heavy residues contain three major fractions: oils, resins and asphaltenes. Asphaltenes are large molecular structures consisting of condensed heterocyclic and aromatic rings, and play a major role in the deactivation of residue processing catalysts by coke. Resins are smaller species with a relatively high degree of aromaticity in the molecule, and are believed to solubilize the asphaltenes in the residue. The oil fraction mainly consists of saturated or unsaturated hydrocarbon chains containing only few heteroatoms. During residue hydroprocessing, oils and resins react more readily than asphaltenes, hence, the concentration of asphaltenes increases until the solubility limit is reached. The surplus of asphaltene molecules will then deposit on the catalyst surface, and eventually be converted into coke [20].

In fixed-bed residue hydroprocessing, multiple reactors are usually applied in series, which are loaded with a selection of catalysts with different functionality. In the first section of the reactor system, the catalyst is exposed to the feed with highest concentration of contaminants and the highest molecular weight. The catalyst that is applied in this position functions mostly as a guard bed and should be able to take up large amounts of V and Ni. Towards the outlet of the reactor system, emphasis is more on hydrodesulfurization and density reduction, while level of contaminants is lower and

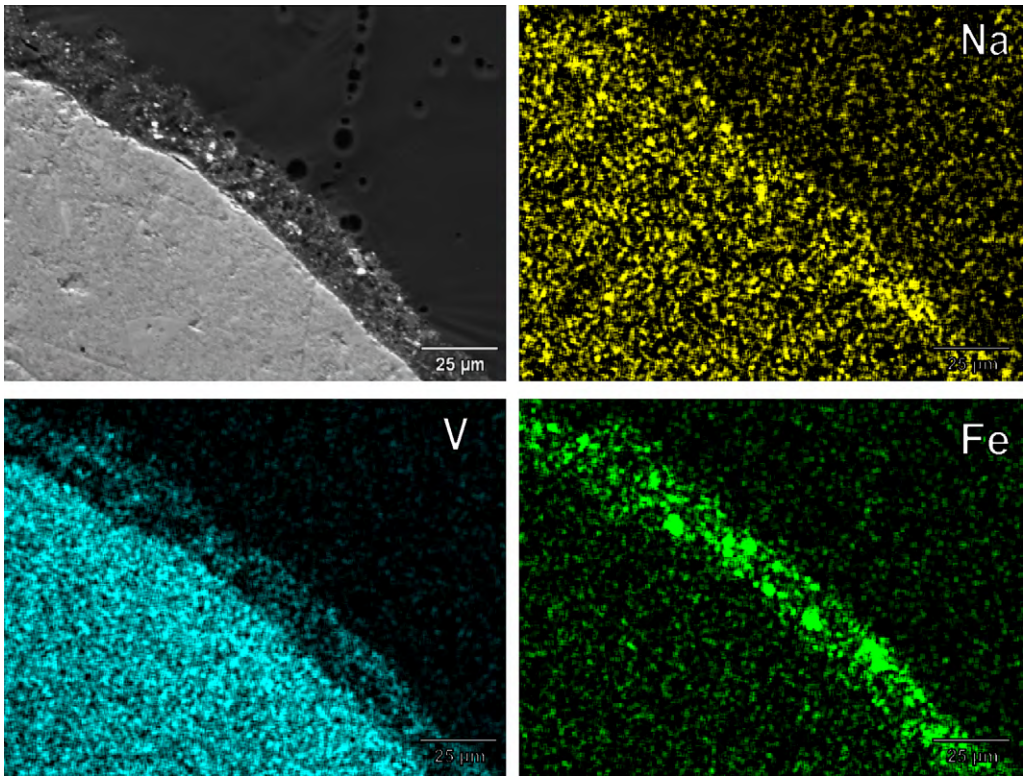

Fig. 7. SEM-EDX of spent Resid HPC catalyst near extrudate surface: new outer layer is formed by Fe deposits.

the size of the molecules has already been reduced. The resistance of a catalyst to pore mouth plugging can be increased by increasing its pore diameter. However, this can only be achieved at the expense of surface area and thus the maximum number of active sites on the catalyst. Hence, for different positions in the reactor, the optimum properties of the catalyst are different. To maximize the hydroprocessing activity and catalyst life cycle of the entire reactor system, the properties of all catalysts need to be optimized [28].

Ebullated bed reactors are applied to process extra heavy vacuum residue fractions under extreme conditions (temperature and pressure). In this case, deactivation is extremely fast and therefore the catalyst is continuously renewed. Since the application of guard bed systems is not possible, ebullated bed catalysts need to be able to withstand the process severity and fouling by contaminants from the feed, while maintaining a certain level of activity. This is often accomplished by designing catalysts with bimodal pore structures [6]. Next to pore plugging, the stability of the active phase is very critical due to the high temperatures applied in residue processing. Therefore, the active phase of residue HPC catalysts is typically stabilized, to prevent the active metals from rapid agglomeration.

Fig. 7 shows the outer edge of a spent residue HPC catalyst pellet from ebullated bed service. Most of the contaminant metals are able to penetrate into the pellet, such as V and Na. However, Fe deposits have formed a layer at the exterior surface of the catalyst. Typically, heavy feeds contain Fe contaminants both in organic structures (e.g. porphyrins) and inorganic particles (oxides and sulfides). These particles cannot enter the catalyst pores and accu-

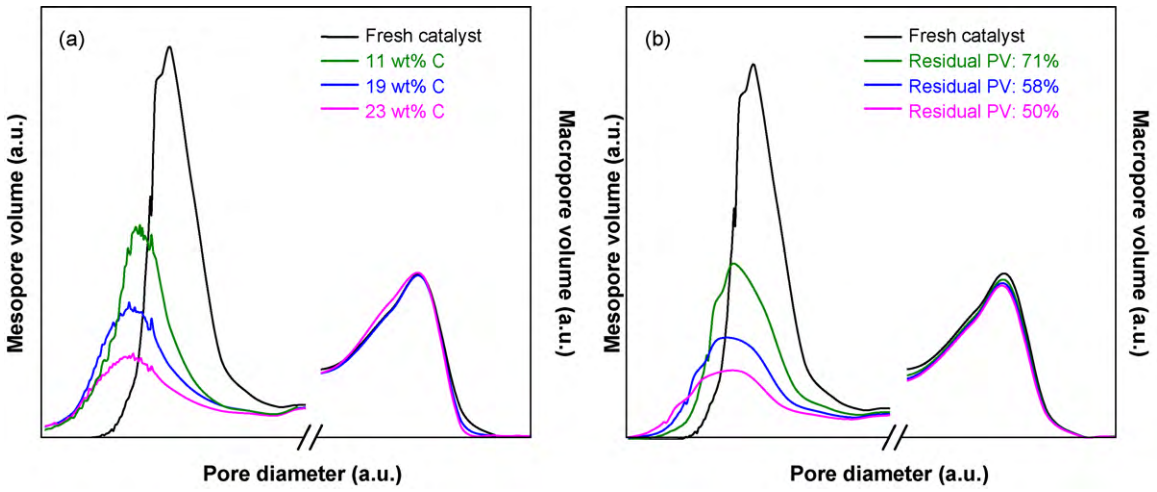

Fig. 8. Spent residue HPC catalyst samples with different time on stream in the reactor: (a) measured and (b) simulated effect of coke deposition on pore size distribution.

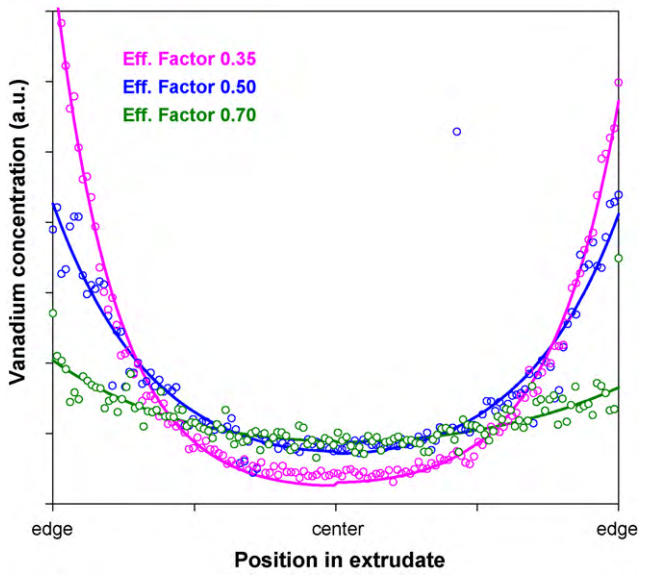

Fig. 9. Vanadium distribution profiles in spent residue HPC catalysts with different metal uptake effectiveness factors.

mulate on the external surface. Furthermore, FeS_x catalyzes coke formation, which may result in rapid pore mouth plugging of the catalyst [2].

The effect of coke and metals deposition on the pore size distribution is shown in Fig. 8. Spent residue HPC catalyst samples were taken at different time on stream from a pilot ebullated bed reactor. The spent catalysts respectively contained 11, 19 and 23 wt% C. The evolution of the measured pore size distributions of the fresh and spent catalysts (Fig. 8a) was fitted with the uniform coking model (Fig. 8b). The model can accurately describe the pore blocking process; the catalyst mesopores are gradually blocked by deposits, whereas the macropores are hardly affected. Apparently, the assumption of equal coke layer thickness is valid; a thin layer of coke on the pore walls hardly changes the diameter and pore volume of the larger pores, in contrast to the smaller pores. This means that the accessibility of catalyst remains high, which reduces the impact of pore blocking on deactivation [29].

Fig. 9 demonstrates the effect of catalyst accessibility on metal uptake efficiency. The distribution of V deposits in three spent catalysts was measured across the pellet cross-section. The resulting V concentration profile was fitted according to a first order diffusion-deposition mechanism, yielding the effectiveness factor for V uptake. At a high effectiveness factor, contaminants are able to penetrate further into the center of the catalyst pellet. At a low effectiveness factor, contaminant deposition will rapidly build-up near the surface of the catalyst particle, resulting in pore mouth plugging [30]. The observed effectiveness factor is a function of accessibility of the catalyst (pore diameter and volume of macropores) and the type of feed that is processed (molar weight and V content). Spent catalyst analysis can thus be used to optimize the catalyst properties for processing of a certain type of feed. These results show the capability of tuning the diffusion-reaction properties of a catalyst pellet in order to custom design the metal trapping properties of the catalyst.

Deactivation mitigation strategies for residue processing in fixed-bed units focus on a balance between metal trapping and catalyst activity. Unlike in VGO units where the main bed is protected by a special guard bed, metal trapping takes place over the entire length of the reactor in fixed-bed residue units. By carefully increasing the catalyst activity from inlet to outlet of the reactor while simultaneously decreasing the metal trapping capacity, the optimal balance between catalyst life and reactor productivity can be designed.

4. Conclusions

Possible causes of catalyst deactivation were identified by analyzing spent catalyst samples from commercial hydroprocessing reactors. Spent catalyst from a commercial diesel HPC unit mainly showed deactivation by coke, whereas catalyst samples applied in an artificial aging procedure at high temperatures exhibited significant loss of dispersion due to sintering of the active metals. Hence, mimicking the industrial life cycle of a catalyst on a laboratory scale is difficult, especially when the conditions used strongly deviate from typical process operation.

The pore structure of used HPC catalysts was significantly altered by coke deposition. The evolution of the pore size distribution could be described using a coking model, assuming an evenly distributed coke layer of uniform thickness on the catalyst surface. Mesopores are most affected by coke deposition, reducing both pore volume and diameter, whereas macropores remain intact.

Metal deposition was observed after hydroprocessing of heavy feeds like VGO and residue, and may be prevented by applying a suitable metal trapping catalyst as guard bed. The impact of coke and metal deposition on deactivation can be minimized by adapting the catalyst pore structure for maximum accessibility.

The studied cases present typical situations of catalyst deactivation that may arise in the commercial practice of hydroprocessing. For each case, dedicated solutions are available to keep the catalyst life cycle under control. Such solutions encompass the optimization of the catalyst system properties, catalyst loading configuration and reactor operation strategy.

References

[1] R.G. Leliveld, S.E. Eijsbouts, How a 70-year-old catalytic refinery process is still ever dependent on innovation, Catal. Today 130 (2008) 183–189.
[2] S. Eijsbouts, A.A. Battiston, G.C. van Leerdam, Life cycle of hydroprocessing catalysts and total catalyst management, Catal. Today 130 (2008) 361–373.
[3] J.A. Moulijn, A.E. van Diepen, F. Kapteijn, Catalyst deactivation: is it predictable? What to do? Appl. Catal. A: Gen. 212 (2001) 3–16.
[4] S.T. Sie, Consequences of catalyst deactivation for process design and operation, Appl. Catal. A: Gen. 212 (2001) 129–151.
[5] C.H. Bartholomew, Mechanisms of catalyst deactivation, Appl. Catal. A: Gen. 212 (2001) 17–60.
[6] E. Furimsky, F.E. Massoth, Deactivation of hydroprocessing catalysts, Catal. Today 52 (1999) 381–495.
[7] B. Delmon, Characterization of catalyst deactivation: industrial and laboratory time scales, Appl. Catal. 15 (1985) 1–16.
[8] J. Ancheyta, G. Betancourt, G. Centeno, G. Marroquín, F. Alonso, E. Garciafigueroa, Catalyst deactivation during hydroprocessing of maya heavy crude oil. 1. Evaluation at constant operating conditions, Energ. Fuel. 16 (2002) 1438–1443.
[9] D. Dong, S. Jeong, F.E. Massoth, Effect of nitrogen compounds on deactivation of hydrotreating catalysts by coke, Catal. Today 37 (1997) 267–275.
[10] J.G. Weissman, J.C. Edwards, Characterization and aging of hydrotreating catalysts exposed to industrial processing conditions, Appl. Catal. A: Gen. 142 (1996) 289–314.
[11] A. Hauser, A. Stanislaus, A. Marafi, Al-Adwani, Initial coke deposition on hydrotreating catalysts. Part II. Structure elucidation of initial coke on hydrodematallation catalysts, Fuel 84 (2005) 259–269.
[12] G.F. Froment, Kinetic modeling of hydrocarbon processing and the effect of catalyst deactivation by coke formation, Catal. Rev. 50 (2008) 1–18.
[13] B.M. Vogelaar, A.D. van Langeveld, S. Eijsbouts, J.A. Moulijn, Analysis of coke deposition profiles in commercial spent hydroprocessing catalysts using Raman spectroscopy, Fuel 86 (2007) 1122–1129.
[14] B. Guichard, M. Roy-Auberger, E. Devers, B. Rebours, A.A. Quoineaud, M. Digne, Characterization of aged hydrotreating catalysts. Part I. Coke depositions, study on the chemical nature and environment, Appl. Catal. A: Gen. 367 (2009) 1–8.
[15] K. Matsushita, A. Hauser, A. Marafi, R. Koidea, A. Stanislaus, Initial coke deposition on hydrotreating catalysts. Part I. Changes in coke properties as a function of time on stream, Fuel 83 (2004) 1031–1038.
[16] S. Eijsbouts, L.C.A. van den Oetelaar, R.R. van Puijenbroek, MoS_2 morphology and promoter segregation in commercial Type 2 Ni–Mo/Al_2O_3 and Co–Mo/Al_2O_3 hydroprocessing catalysts, J. Catal. 229 (2005) 352–364.

[17] P.J. Kooyman, J.G. Buglass, H.R. Reinhoudt, A.D. van Langeveld, E.J.M. Hensen, H.W. Zandbergen, J.A.R. van Veen, Quasi in situ sequential sulfidation of $CoMo/Al_2O_3$ studied using high-resolution electron microscopy, J. Phys. Chem. B 106 (2002) 11795–11799.
[18] Y. Tanaka, H. Shimada, N. Matsubayashi, A. Nishijima, M. Nomura, Accelerated deactivation of hydrotreating catalysts: comparison to long-term deactivation in a commercial plant, Catal. Today 45 (1998) 319–325.
[19] R.R. Galiasso Tailleur, Catalyst deactivation during upgrade of light catalytic cracking gas oil to ultralow-sulfur and low-aromatic diesel, Energ. Fuel. 22 (2008) 1509–1518.
[20] D.L. Trimm, Deactivation, regeneration and disposal of hydroprocessing catalysts, Stud. Surf. Sci. Catal. 53 (1990) 41–60.
[21] C.H. Bartholomew, Catalyst deactivation in hydrotreating of residua: a review, Chem. Ind. 58 (1994) 1–32.
[22] M. Baghalha, S.M. Hoseini, Long-term deactivation of a commercial $CoMo/\gamma$-Al_2O_3 catalyst in hydrodesulfurization of a naphtha stream, Ind. Eng. Chem. Res. 48 (2009) 3331–3340.
[23] M.A. Callejas, M.T. Martínez, J.L.G. Fierro, C. Rial, J.M. Jiménez-Mateos, F.J. Gómez-García, Structural and morphological study of metal deposition on an aged hydrotreating catalyst, Appl. Catal. A: Gen. 220 (2001) 93–104.
[24] B.J. Smith, J. Wei, Deactivation in catalytic hydrodemetallation II. Catalyst characterization, J. Catal. 132 (1991) 21–40.
[25] E.K.T. Kam, M. Al-Shamali, M. Juraidan, H. Qabazard, A hydroprocessing multicatalyst deactivation and reactor performance model – pilot-plant life test applications, Energ. Fuel. 19 (2005) 753–764.
[26] F. Díez, B.C. Gates, J.T. Miller, D.J. Sajkowski, S.G. Kukes, Deactivation of a $Ni–Mo/\gamma$-Al_2O_3 catalyst: influence of coke on the hydroprocessing activity, Ind. Eng. Chem. Res. 29 (1990) 1999–2004.
[27] K.P. De Jong, H.P.C.E. Kuipers, J.A.R. Van Veen, Topology of coke deposits in spent heavy oil processing catalysts. A quantitative X-ray photoelectron spectroscopy study, Stud. Surf. Sci. Catal. 68 (1991) 289–296.
[28] J.G. Speight, New approaches to hydroprocessing, Catal. Today 98 (2004) 55–60.
[29] P. Zeuthen, J. Bartholdy, P. Wiwel, B.H. Cooper, Formation of coke on hydrotreating catalysts and its effect on activity, Stud. Surf. Sci. Catal. 88 (1994) 199–206.
[30] M.C. Tsai, Y.W. Chen, C. Li, Restrictive diffusion under hydrotreating reactions of heavy residue oils in a trickle bed reactor, Ind. Eng. Chem. Res. 32 (1993) 1603–1609.